

# Symbolic dynamics of the stadium billiard

Wei-Mou Zheng

*Institute of Theoretical Physics, Academia Sinica, Beijing 100080, China*

(Received 15 January 1997)

By viewing the stadium billiard as a map on the annulus, codes are introduced for both the full and half stadium based on the lift. By means of such codes, the symbolic dynamics of stadium is described. The relation of the codes to other codes is discussed. [S1063-651X(97)06208-9]

PACS number(s): 05.45.+b, 03.20.+i

## I. INTRODUCTION

The stadium billiard introduced by Bunimovich is a model of complete chaos [1]. The boundary of the billiard consists of two semicircles of radius 1 joined by two straight segments of length  $2a$ . A point particle moves freely in the interior of the billiard and elastically reflects from the boundary upon collision. The quantum mechanics of the stadium billiard as a system being chaotic in the classical limit has also received much attention [2]. Many eigenfunctions of the quantized stadium billiard have patterns of strong enhancement in probability amplitude showing scars of classical unstable periodic orbits [3].

In Ref. [4] Biham and Kvale introduced a symbolic dynamics for the stadium that associates each orbit with a unique symbolic sequence. Later Hansen and Cvitanović [5] developed a more compact, desymmetrized covering symbolic dynamics. Meiss [6] explored ordered periodic orbits and cantori classified with rotation numbers. By means of the arc length  $s$  along the boundary and the tangent component  $v$  of the momentum, i.e., the Birkhoff coordinates, a map of the annulus is generated from the stadium. The dynamics of the map may be better understood by lifting and then wrapping. In this way we can study the orientation and rotation numbers of orbits. The information about the rotation number of an orbit is not explicitly contained in the Biham-Kvale (BK) coding or Hansen-Cvitanović (HC) coding. In this paper we propose another coding based on lifting. We shall introduce the coding in the next section. This coding will be compared with other codings in Sec. III. In Sec. IV we apply the same idea to the half stadium. The limit of an infinite long flat wall is treated in Sec. V. Finally, in Sec. VI we make a few concluding remarks.

## II. A CODING BASED ON LIFTING

We measure the arc length of the boundary along the counterclockwise direction from the lower end of the left semicircle, i.e., at that joint point  $s=0$ , and denote by  $L$  the half length  $\pi+2a$  of the boundary. The annulus corresponds to the fundamental domain (FD) of  $s \in [0, 2L)$  and  $v \in [-1, 1]$ . The image and preimage of this domain in the lifted space are shown in Figs. 1 and 2, respectively. The area  $hij$  of the FD shown in Fig. 2 (to the right of the curve connecting points  $i$  and  $j$ ) maps to the area  $bcd$  to the right of the FD shown in Fig. 1 under the forward map, while the area  $fbe$  of Fig. 1 (to the left of the lower curve connecting

points  $b$  and  $e$ ) maps to the area  $g lk$  of Fig. 2 to the left of the FD. It is known that a bounce off a straight wall reverses the ordering of two neighboring orbits, while a bounce off a semicircle preserves the ordering [5]. Thus the four strips separated by lines  $s=2a, s=L$ , and  $s=L+2a$  in the FD of Fig. 2 must be assigned different symbols. To reflect the different behavior in the lifted map, we further divide the FD with the preimage curve  $hj$  of the line  $s=0$ . In this way we partition the FD into seven pieces assigned symbols  $M, L, L_1, N, N_1, R$ , and  $R_1$  as shown in Fig. 2. This seven-letter alphabet shall be called the full stadium (FS) code later on. By means of this partition we may code an orbit with a doubly infinite sequence

$$\cdots s_{-1} \bullet s_0 s_1 \cdots,$$

where  $\bullet$  indicates the present. The corresponding partition according to preimages is shown in Fig. 1, where each piece is the image of its counterpart in Fig. 2. For example,  $L_1 \bullet$  is the image of  $\bullet L_1$ , where we have used  $\bullet$  to distinguish the two different partitions. Since the image and preimage advance in opposite directions,  $L_1 \bullet$  is an area to the left of the FD in the lifted space.

We may accept the natural order of the lifted space to write

$$L_1 \bullet < N_1 \bullet < R_1 \bullet < M \bullet < L \bullet < N \bullet < R \bullet \quad (1)$$

since their preimages are arranged successively from left to right in the lifted space. To compare two backward se-

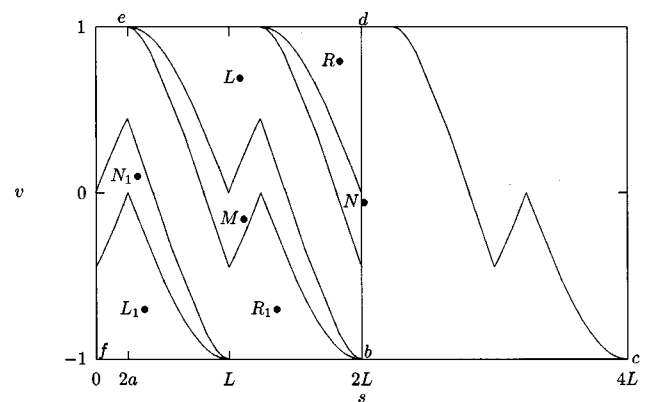


FIG. 1. Image  $bcde$  of the fundamental domain  $s \in [0, 2L)$  and  $v \in [-1, 1]$  and the partition of the domain according to preimages of orbit points for  $a=0.5$  (cf. Fig. 2).

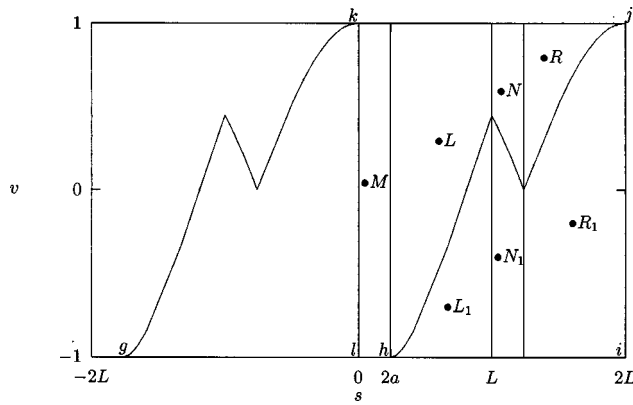


FIG. 2. Preimage  $ghjk$  of the fundamental domain and the partition of the domain according to the present point for  $a=0.5$  (cf. Fig. 1).

quences we need the definition of parity for a finite string that is the oddness of the total number of the symbols  $M, N$ , and  $N_1$  contained in the string. Any odd leading string will reverse the above ordering.

The same principle may be applied to the ordering of forward sequences. We have  $\bullet M < \{\bullet L, \bullet L_1\} < \{\bullet N, \bullet N_1\} < \{\bullet R, \bullet R_1\}$ . While the image of  $\bullet L$  stays in the FD, that of  $\bullet L_1$  is located to the right of the FD. Since  $L$  and  $L_1$  preserve the ordering of neighboring orbits, according to their image we have  $\bullet L < \bullet L_1$ . Similarly,  $\bullet R < \bullet R_1$ . Taking into account the fact that  $N$  and  $N_1$  reverse the ordering, we have  $\bullet N_1 < \bullet N$ . In summary, the ordering rule for forward sequences is

$$\bullet M < \bullet L < \bullet L_1 < \bullet N_1 < \bullet N < \bullet R < \bullet R_1. \quad (2)$$

Similarly, an odd leading string will also reverse this ordering.

Based on the ordering rules, metric representations for both forward and backward sequences may be introduced to construct the symbolic plane [7]. Every forward or backward sequence then corresponds to a number between 0 and 1. An orbit point corresponds to a point  $(\alpha, \beta)$  in the unit square, where  $\alpha$  and  $\beta$  are associated with the forward and backward sequences, respectively. In the symbolic plane forbidden sequences are pruned by the so-called primary pruning front, which consists of the points in the symbolic plane representing all the points on the partition lines ( $s=0, s=2a, s=L$ , and  $s=L+2a$ ). As an example, we show the symbolic plane for  $a=0.5$  in Fig. 3, where 15 000 points of several real orbits are drawn. The corresponding primary pruning front is shown in Fig. 4.

The above coding, describing the dynamics of lifting and wrapping, directly gives the rotation number of a periodic orbit as the total number of symbols with subscript 1 in the nonrepeating string of its symbolic sequence divided by the length of the string. For the orientation-preserving circle map symbols with subscript 1 must be greater than any symbols without a subscript 1 [8]. According to relation (2), this is possible only when

$$\bullet M < \bullet L < \bullet N < \bullet R < \bullet R_1$$

or

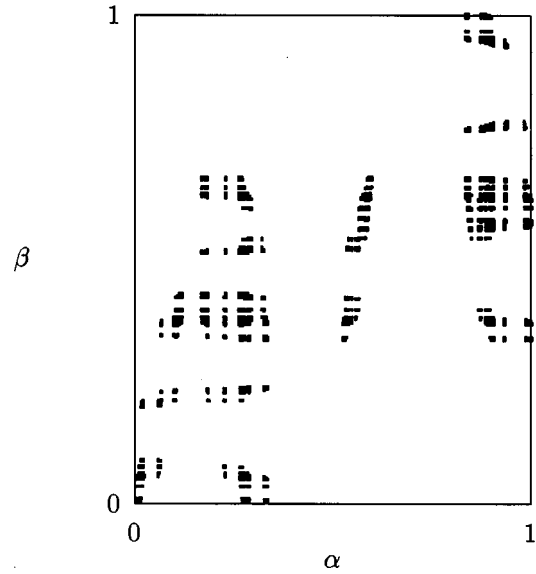


FIG. 3. Symbolic plane for  $a=0.5$ . Approximately 15 000 real orbit points are drawn.

$$\bullet M < \bullet L < \bullet L_1 < \bullet N_1 < \bullet R_1.$$

So an orientation-preserving orbit consists of at most five letters, belonging to one of the two categories. In this way the ordering for backward and forward sequences coincides. In both cases  $M, N$ , or  $N_1$  appears at most once, except for periodic orbits. This implies the nonexistence of invariant circles for  $a \neq 0$ . Furthermore, when two different symbols  $t$  and  $t'$  are both with or without a subscript 1 and satisfy  $t > t'$ , then any subsequence following  $t$  is never smaller than any sequence following  $t'$ . Any subsequence following a letter with subscript 1 is never greater than any subsequence following a letter without subscript 1. For example, the two  $(1,3)$  orbits shown in Fig. 4 of Ref. [6] are  $(LLLRRR_1)^\infty$  and  $(MLLNRR_1)^\infty$ . Two examples of orientation-preserving infinite sequences are  $(LRR_1L)^\infty(RR_1LL)^\infty$  and  $(LRR_1L)^\infty NR_1M(LRR_1L)^\infty$ .

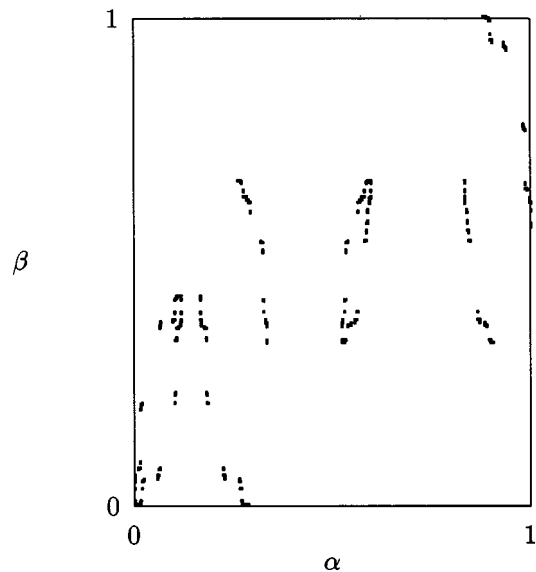


FIG. 4. Primary pruning front for  $a=0.5$ . It forms the border of the region within which orbit points are restricted to fall.

### III. RELATION TO OTHER CODINGS

The BK code associates a bounce with a six-letter alphabet  $\{0,1,2,3,4,5\}$  defined as follows: 0 is a bounce off the bottom wall, 1 a clockwise bounce off the left semicircle or a single counterclockwise bounce off the left semicircle, 2 a bounce off the top wall, 3 a counterclockwise bounce off the right semicircle or a single clockwise bounce off the right semicircle, 4 a nonsingle counterclockwise bounce off the left semicircle, and 5 a nonsingle clockwise bounce off the right semicircle. In the FS code the arc length is allowed to continue to increase past  $2L$ . In this way a forward orbit always advances forward in the lifted space. Thus a point should be coded by a symbol with subscript 1 if its image has an  $s$  smaller than itself in the FD. The correspondence from the BK code to the FS code is then as follows: 0 corresponds to  $M$ ,  $2(\{1,4\})$  to  $N$ ,  $2(\{0,3,5\})$  to  $N_1$ ,  $3(\{2,3,1,4\})$  and  $5(\{2,1,4\})$  to  $L$ ,  $3(0)$  and  $5(\{0,5\})$  to  $L_1$ ,  $4(4)$  to  $R$ , 1 and  $4(\{0,2,3,5\})$  to  $R_1$ , where we have used the fact that 14, 41, 35, and 53 are forbidden [4]. For example,  $(0321)^\infty$  corresponds to  $(MLNR_1)^\infty$ ,  $(3212)^\infty$  to  $(LNR_1N_1)^\infty$ , and  $(055211)^\infty$  to  $(ML_1LNR_1R_1)^\infty$ .

The definition of a single bounce depends on the preceding or following bounce, while the FS code depends only on the present bounce. It can be verified that the correspondence from the FS code to the BK code is as follows:  $\bullet M$  corresponds to 0,  $\bullet N$  and  $\bullet N_1$  to 2,  $(L_1) \bullet \{L, L_1\}$  and  $\bullet L_1 \{L, L_1\}$  to 5,  $\bullet L_1(M)$  and  $(\{N_1, R_1, M, L\}) \bullet L$  to 3,  $(R) \bullet$  and  $\bullet R$  to 4, and  $(\{R_1, M, L, N\}) \bullet R_1$  to 1, where we have indicated a preceding or following bounce with a parenthesis. For example,  $(LLLRRR_1)^\infty$  corresponds to  $(333444)^\infty$  and  $(MLLNRR_1)^\infty$  to  $(033244)^\infty$ .

Overlapping the FD in Figs. 1 and 2, one can see that the allowed pairs of symbols are  $M\{L, L_1, N, N_1, R, R_1\}$ ,  $L\{L, L_1, N, N_1, R, R_1\}$ ,  $L_1\{M, L, L_1\}$ ,  $N\{R, R_1\}$ ,  $N_1\{M, L, L_1\}$ ,  $R\{R, R_1\}$ , and  $R_1\{M, L, L_1, N_1, R_1\}$ . Written in an equivalent way, these pairs are  $\{L_1, N_1, R_1\}M$ ,  $\{M, L, L_1, N_1, R_1\}L$ ,  $\{M, L, L_1, N_1, R_1\}L_1$ ,  $\{M, L\}N$ ,  $\{M, L, R_1\}N_1$ ,  $\{M, L, N, R\}R$ , and  $\{M, L, N, R, R_1\}R_1$ . There are 22 forbidden pairs.

In Ref. [5] the HC code, which is a symmetry reduced five-letter alphabet, was introduced by defining  $\bar{0}$  as a first bounce off either semicircle,  $\bar{1}$  a clockwise nonfirst bounce off a given semicircle,  $\bar{2}$  a counterclockwise nonfirst bounce off a given semicircle,  $\bar{3}$  a bounce off a flat wall with positive  $v$ , and  $\bar{4}$  a bounce off a flat wall with negative  $v$ . It can be verified that the correspondence between this code and the FS code is as follows:  $\bar{0}$  corresponds to  $\{M, N_1, R_1\} \bullet L$ ,  $\{M, N_1, R_1\} \bullet L_1$ ,  $\{M, L, N\} \bullet R$ , and  $\{M, L, N\} \bullet R_1$ ,  $\bar{1}$  to  $L_1 \bullet L, L_1 \bullet L_1$ , and  $R_1 \bullet R_1$ ,  $\bar{2}$  to  $L \bullet L, L \bullet L_1, R \bullet R$ , and  $R \bullet R_1$ ,  $\bar{3}$  to  $\{R_1, N_1^+\} \bullet M$ ,  $\{M, L\} \bullet N$ , and  $\{L, M^+\} \bullet N_1$ ; and  $\bar{4}$  to  $\{L_1, N_1^-\} \bullet M$  and  $\{M^-, R_1\} \bullet N_1$ , where by  $M^+$  ( $M^-$ ) we mean a backward sequence greater (smaller) than  $(N_1M)^\infty$  and by  $N_1^+$  ( $N_1^-$ ) a sequence greater (smaller) than  $(MN_1)^\infty$ . In fact, this five-letter code is for the half stadium [5]. We shall discuss the half stadium further in the next section.

### IV. THE HALF STADIUM

The stadium map has the translation symmetry to be invariant under  $(s, v) \rightarrow (s-L, v)$ , which may be used to re-

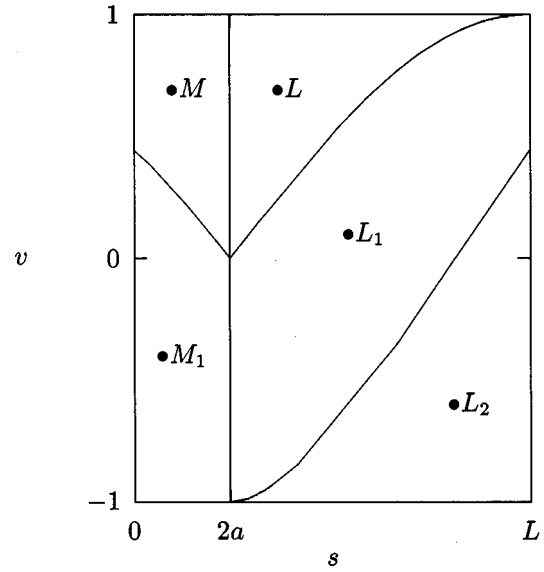


FIG. 5. Partition of the phase space for the half stadium with  $a=0.5$  according to the present point.

duce the motion to the half domain [6]. We may partition the phase space of this half stadium in a way similar to that for the full stadium. The partition is shown in Fig. 5. The phase space is divided into  $\bullet M, \bullet M_1, \bullet L, \bullet L_1$ , and  $\bullet L_2$  by the line  $s=2a$  and the two-piece preimage of the line  $s=0$ . The corresponding partition according to the past  $M \bullet, M_1 \bullet, L \bullet, L_1 \bullet$ , and  $L_2 \bullet$  is shown in Fig. 6. This five-letter alphabet shall be referred to as the half stadium (HS) code. It can be verified that the correspondence between the HS and FS codes is as follows:  $M$  in the five-letter code corresponds to  $\bullet M\{L, L_1\}$ , and  $\bullet N$  in the seven-letter code,  $M_1$  to  $\bullet M\{N, N_1, R, R_1\}$ , and  $\bullet N_1$  to  $\bullet L\{L, L_1\}$ , and  $\bullet R\{R, R_1\}$ ,  $L_1$  to  $\bullet L\{N, N_1, R, R_1\}$ , and  $\bullet R_1\{M, L, L_1\}$ , and  $L_2$  to  $\bullet L_1\{M, L, L_1\}$ , and  $\bullet R_1\{N_1, R_1\}$ .

Using the same argument to obtain the ordering of the seven symbols for the full stadium, we have similarly the ordering

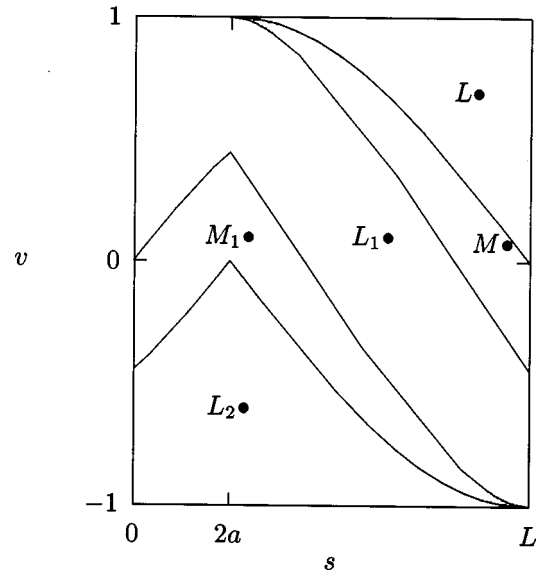


FIG. 6. Partition of the phase space for the half stadium with  $a=0.5$  according to the preimage of the present point.

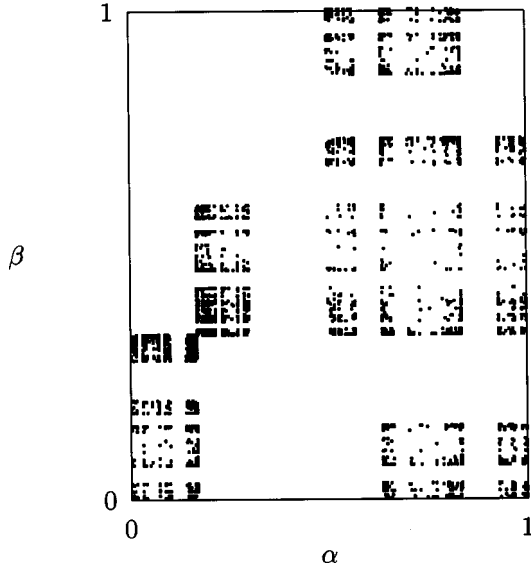


FIG. 7. Symbolic plane of the half stadium at  $a=5$ . Approximately 15 000 real orbit points are drawn.

$$L_2 \bullet < M_1 \bullet < L_1 \bullet < M \bullet < L \bullet, \quad (3)$$

$$\bullet M_1 < \bullet M < \bullet L < \bullet L_1 < \bullet L_2. \quad (4)$$

Similarly, a symbol  $M$  or  $M_1$  will reverse the order of forward or backward sequences, while  $L, L_1$ , and  $L_2$  preserve the order. We can also construct the symbolic plane for the half stadium. The symbolic plane for  $a=5$  is shown in Fig. 7, where 15 000 points of several real orbits are drawn. The corresponding primary pruning front is shown in Fig. 8.

Either from Figs. 5 and 6 or from Fig. 7, we see that in the HS code 6 symbol pairs  $LM_1, LM, MM_1, MM, L_2M$ , and  $L_2L$  are forbidden. The HS code excludes many forbidden symbol pairs of the FS code at the beginning, hence is more compact. Forbidden pairs of the HS code correspond to forbidden triplets of the FS code, so they contain some information about pruning. For example, the forbidden  $L_2L$  of the HS code implies the forbidden  $L_1ML, L_1ML_1, L_1LL$ , and  $L_1LL_1$  of the FS code.

## V. THE LIMIT OF INFINITE $a$

The main ingredients of symbolic dynamics are the foliation of the phase space by stable and unstable manifolds, the geometric relation between the two kinds of manifolds, partition of the phase space, and monotonic ordering in the symbolic coding for both kinds of manifolds. In the construction of the primary pruning front every point on a partition line maps to a point in the symbolic plane that forms a vertex of a forbidden rectangle in the plane. Generally, such a pruning front consists of an infinite number of vertices. However, in limiting cases, e.g., the limit of infinite  $a$ , the number of vertices may reduce to finite one.

For the FS code in the limit  $a \rightarrow \infty$  the finite vertices are  $(MN_1)^\infty \bullet (MN_1)^\infty$ ,  $R^\infty R_1 \bullet ML^\infty$ ,  $R^\infty R_1 \bullet L^\infty$ ,  $(MN_1)^\infty \bullet L(N_1M)^\infty$ ,  $L^\infty \bullet LR_1^\infty$ ,  $L^\infty \bullet L_1(MN_1)^\infty$ ,  $(R_1)^\infty \bullet L_1^\infty R_1^\infty N_1 L_1^\infty$ ,  $(N_1M)^\infty \bullet (N_1M)^\infty$ ,  $L^\infty \bullet NR_1^\infty$ ,  $L^\infty \bullet R^\infty$ ,  $(N_1M)^\infty \bullet R_1(MN_1)^\infty$ ,  $R_1^\infty \bullet R_1 L_1^\infty$ , and  $(N_1M)^\infty \bullet N \bullet R_1(N_1M)^\infty$ . For the HS code the number of the vertices is greatly reduced. These

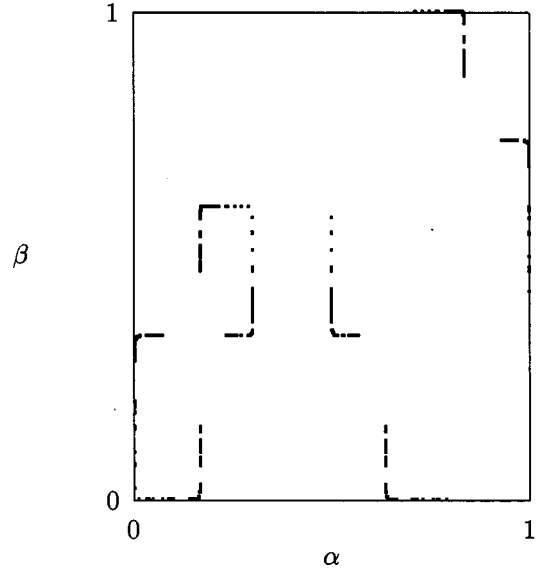


FIG. 8. Primary pruning front of the half stadium at  $a=5$ . It forms the border of the region within which orbit points are restricted to fall.

vertices are  $M_1^\infty \bullet M_1^\infty$ ,  $L^\infty L_1 \bullet ML^\infty$ ,  $L^\infty L_1 \bullet L^\infty$ ,  $M_1^\infty \bullet L_1 M_1^\infty$ , and  $M_1^\infty \bullet L_2 M_1^\infty$ . They correspond to their counterparts in the FS code, but some vertices of the FS code, e.g.,  $R_1^\infty \bullet R_1 L_1^\infty$  (converted to  $L_2^\infty \bullet L_1 L_2^\infty$ ), become trivial. The five vertices give a complete description of the geometric pruning that holds for all values of the parameter  $a$ .

## VI. CONCLUSION

In the previous sections we have obtained a simple partition of the phase space for both the full and half stadium billiard based on the lift. The ordering rules for the stadium are essentially the same as those for the dissipative standard map [9]. The rigorous proofs concerning ordering involve the global dynamical properties of the system and no such proofs are available yet.

The arguments may be applied to other systems such as the  $n$ -disk pinballs. In Hamiltonian systems we often deal with angle variables. A lift of the phase space helps us to understand the dynamics. The symbolic dynamics of the stadium billiard is as simple as the piecewise linear standard map [10] in the sense that the partition lines are given by the definition of the map at the beginning.

The symbolic dynamics will enable us to predict all the possible motions, including not only periodic, but also chaotic orbits. By means of the simple codes we may further discuss metric properties as well as topological ones.

The coding based on the lifting contains direct information about the rotation number and orientation. Orbits with different orientation-preserving properties might play different roles in forming scars of the quantized billiard. In this case the above FS and HS codes would be useful.

## ACKNOWLEDGMENTS

The author thanks Hao Bai-lin and K. T. Hansen for useful discussions. This work was supported in part by the National Natural Science Foundation of China.

- [1] L. A. Bunimovich, *Funct. Anal. Appl.* **8**, 254 (1974); *Commun. Math. Phys.* **65**, 295 (1979).
- [2] S. W. McDonald and A. N. Kaufman, *Phys. Rev. Lett.* **42**, 1189 (1979).
- [3] E. J. Heller, *Phys. Rev. Lett.* **53**, 1515 (1984).
- [4] O. Biham and M. Kvale, *Phys. Rev. A* **46**, 6334 (1992).
- [5] K. T. Hansen and P. Cvitanović (unpublished).
- [6] J. D. Meiss, *CHAOS* **2**, 267 (1992).
- [7] P. Cvitanović, G. H. Gunaratne, and I. Procaccia, *Phys. Rev. A* **38**, 1503 (1988).
- [8] W. M. Zheng, *Int. J. Mod. Phys. B* **5**, 481 (1991); *Chaos Solitons Fractals* **4**, 1221 (1994).
- [9] W. M. Zheng, *Commun. Theor. Phys.* (to be published).
- [10] S. Bullett, *Commun. Math. Phys.* **107**, 241 (1986).